

Guided Visual Attention Model Based on Interactions Between Top-down and Bottom-up Prediction for Robot Pose Prediction

Hyogo Hiruma

*Department of Intermedia Art and Science
Fundamental Science and Engineering
Waseda University
Tokyo, Japan
hiruma@idr.ias.sci.waseda.ac.jp*

Hiroki Mori

*Future Robotics Organization
Waseda University
Tokyo, Japan
mori@idr.ias.sci.waseda.ac.jp*

Hiroshi Ito

*Controls and Robotics
Center for Technology Innovation
Research & Development Group
Hitachi, Ltd.
Ibaraki, Japan
hiroshi.ito.ws@hitachi.com*

Tetsuya Ogata

*Department of Intermedia Art and Science
Fundamental Science and Engineering
Waseda University,
National Institute of Advanced
Industrial Science and Technology (AIST)
Tokyo, Japan
ogata@waseda.jp*

Abstract—Deep robot vision models are widely used for recognizing objects from camera images, but shows poor performance when detecting objects at untrained positions. Although such problem can be alleviated by training with large datasets, the dataset collection cost cannot be ignored. Existing visual attention models tackled the problem by employing a data efficient structure which learns to extract task relevant image areas. However, since the models cannot modify attention targets after training, it is difficult to apply to dynamically changing tasks. This paper proposed a novel Key-Query-Value formulated visual attention model. This model is capable of switching attention targets by externally modifying the Query representations, namely top-down attention. The proposed model is experimented on a simulator and a real-world environment. The model was compared to existing end-to-end robot vision models in the simulator experiments, showing higher performance and data efficiency. In the real-world robot experiments, the model showed high precision along with its scalability and extendibility.

Index Terms—neural networks, robotics, visual attention

I. INTRODUCTION

Robot task learning incorporating end-to-end learned vision models enables flexible recognition of complex environments; but has long suffered by the requirement for large training datasets. Inspired by the dominant attention models in natural language processing [1], recent studies apply the unique structure for various purposes, including image recognition [2]–[4] and robot vision processing [5]–[7]. Attention models for robot vision are designed to reduce the required dataset size by employing a structure that extracts target data from task relevant image areas. However, most of such structures

have limitations, in which the attention targets are intended to be fixed throughout the task. As real-world robot applications often handle multiple type of objects, the ability to direct attention to different targets on demand is indispensable.

Originally, attention mechanisms are human cognitive activity to selectively extract necessary information from innumerable number of stimuli. Generally, it is considered as an integrated system composed of “bottom-up attention” and “top-down attention” [8]. The bottom-up attention automatically collects stimuli of conspicuous areas of the visual receptive field. By contrast, the top-down attention biases/filters out from the collected stimuli and selectively extracts a target.

In machine learning, most existing models only consist of visual bottom-up attention. Although some previous works incorporated controllable visual attention models [7], [9], they possess structural weaknesses that limit application areas and interpretability. The lack of interpretability is considered to be an critical issue for future robot applications, such as human-robot collaboration [10], [11].

This work proposed a novel visual attention model, which is capable of controlling attention targets in a top-down manner. The model was trained and evaluated on a simulator and real-world environment robot tasks. The tasks included picking top-down specified objects, which the model succeeded by inputting extra conditions that explicitly specify the attention targets. In addition, the simulator results showed the model’s characteristics of high data efficiency, interpretability, and robustness against appearance changes.

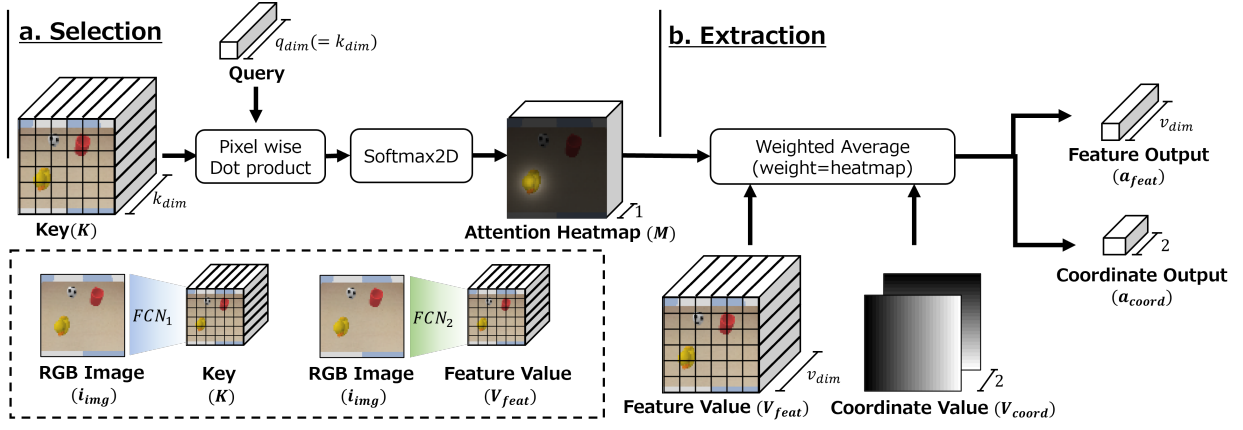


Fig. 1. Abstract of visual attention model. (a) Selection phase: Generates attention heatmap. Scans through the Key and search for the area that matches the Query vector. The heatmap is computed by the scaled dot product of the Query vector and the feature vector at each pixel of the Key. (b) Extraction phase: Selectively extracts feature vectors and coordinates on attended positions. FCN_1 and FCN_2 do not share the weights.

II. RELATED WORKS

A. Visual processing for robots

Recognizing object's location and orientation from visual input is an inevitable task in robot applications. This especially applies for environment interaction or object manipulation purposes. Studies have tackled this task by acquiring object-centric representations through various methods, such as object detection [12], [13], key point prediction [14], [15], and 3D pose estimation [16], [17]. However, all the methods require a specially labeled dataset and suffer from its collection cost.

Other studies eliminated the need of specific labels by employing end-to-end robot task learning [18], [19], using vanilla Fully Convolutional Networks (FCN). End-to-end learning enables implicit acquisition of object-centric representations, by learning to directly map input images and predictions [18]. Despite the elimination of labels, the copious amount of data required still enlarges the dataset collection cost. One major cause is the computational nature of FCNs [20], where the extracted image features cannot carry the information of where it originated within the input image. Although it is possible to acquire some positional information through training, it requires image datasets with objects placed at various positions. This increases the dataset size, hence suffer from the collection cost.

B. Visual attention for robots

Recent robot vision models [5], [6], [21] utilize attention structures to improve data efficiency. Through end-to-end learning, attention models learn to predict heatmaps which is composed of attention weights of each image pixels. The predicted weights tend to illuminate task relevant targets, such as target objects. In robot tasks, attention models explicitly extracts the pixel coordinates of where the objects are located. This eliminates the need of empirically acquiring spatial representations, and contributes in dataset size reduction.

However, the mentioned visual attention models only employ bottom-up attention, which cannot modify the attention

targets after fixing the model weights. Although some studies [7], [9] extended the model to incorporate top-down attentions, they have limitations. Spatial Attention Point Networks [9] enabled top-down control by implicitly filtering out from a redundant number of attention points. Although the model can control the attention by switching input conditions, the implicit filtering reduced the model's interpretability. By contrast, the proposed model predicts on a minimum number of attention points to retain interpretability, where the targets of each attention points can be modified by specifying with external inputs.

III. MODEL ARCHITECTURE

A. Spatial attention mechanism

The proposed attention mechanism model acquires attention through end-to-end learning, without any explicit supervisions of where or what to attend to. As shown in Fig. 1, the model is constructed using the Key-Query-Value structure [1], and comprises of two phases: a selection phase (Fig. 1 (a)) and an extraction phase (Fig. 1 (b)). This model can easily be expanded to multi-head attention by learning multiple weights in parallel. The following sections will describe the architecture of the selection and extraction phases.

B. Selection phase

The selection phase scans and predicts the attention weights of each image pixels. A Key representation K is an image feature of input image i_{img} extracted by a FCN (FCN_1). FCN_1 is a three layered convolutional network with positional embedding concatenated and applied after each layer as in [20]. The model computes pixel-wise dot product of K and a Query vector Q , and applies 2D softmax with temperature. Q represents an image feature of the attention target. Such a representation is learned simultaneously by end-to-end learning; this will be discussed in the later sections. The output is the attention heatmap M , with large weights at pixels where K had image features that are similar to the Q vector.

$$M = \text{Softmax}_{2D} \left(\frac{K \odot Q}{\sqrt{HW}} \right) \quad (1)$$

H and W represents the height and width of image feature K . \odot stands for pixel-wise scaled dot product [1]. During above operation, the roles of K and Q are to mutually interact to construct task relevant representations. In this sense, K and Q act as the bottom-up and top-down attention, respectively.

C. Extraction phase

The extraction phase extracts the image feature and coordinate of attended locations, in reference to M . First, the model generates two Value representations that spatially correspond to M : Feature Value V_{feat} and Coordinate Value V_{coord} . V_{feat} is an image feature of the input image, converted with FCN_2 which does not share weights with FCN_1 . V_{coord} is an absolute positional embedding which lists the coordinate values of each pixel in image format. For simplicity, this model employs a Cartesian coordinate embedding which lists x and y coordinates in two different channels.

Given these value representations, the model calculates a weighted average through spatial dimension, or expectation operation as referred to in [5]. The outputs are treated as the selective extraction of the attention model: target feature vector a_{feat} and target coordinate a_{coord} . The extracted data will contain values that are close to those that originated at the attended pixels, since $M \in [0.0, 1.0]$. (u, v) represents the position of each pixels.

$$a_{feat} = \sum_{u=0}^W \sum_{v=0}^H M_{(u,v)} V_{feat(u,v)} \quad (2)$$

$$a_{coord} = \sum_{u=0}^W \sum_{v=0}^H M_{(u,v)} V_{coord(u,v)} \quad (3)$$

D. Query vector generation and top-down attention

One strength of the proposed model is that it is structured to store object-centric representations in a distinct variable Q , which existing models cannot. This allows the model to modify the attention targets by switching Q s with corresponding representations. Such Q s can be created in various ways, depending on the task. This subsection will describe two methods.

1) *Base Query*: A simple implementation is to use learnable variables as Q s. The variables are initialized with random values and are trained to store target object representations; we term such a variable as Base Queries q_n^B . Multiple Base Queries can be learned simultaneously and be manually switched on inference. This way, one can modify the attention targets in a top-down manner.

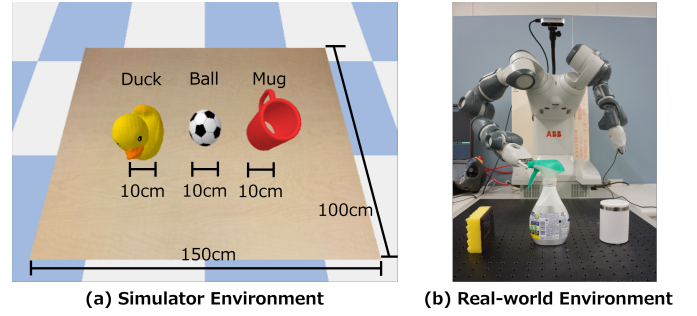


Fig. 2. Environments: (a) A simulator environment running on PyBullet, including three types of figures. (b) Real-world environment contains a 7DOF dual-arm robot with three types of objects.

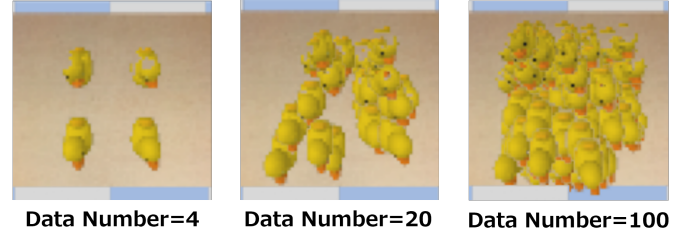


Fig. 3. Relation of positional density and dataset size. Each image displays the total area and density covered by the object. The dataset is based on a task (a). Above images are rendered for visualization.

TABLE I
EXPERIMENT TASK CONFIGURATIONS

Task name	Number of Presented Objects	Number of Target Objects	Top-down Specification
(a) Single Object	1	1	-
(b) Multiple Object	3	3	-
(c) Selected Type	3	1	Object type
(d) Selected Position	2	1	Object Position

2) *Conditioned Query*: Conditioned Queries are Queries created based on additional input conditions c_{query} . The conditions include one-hot vectors, images, natural language embeddings, which are embedded to vector representations using multi-layer perceptrons (MLP). This can be combined with Base Queries, for learning different targets with similar appearances (e.g. attending to one of identical objects based on their positions). The Base Queries will store the major visual characteristics and the conditions will support to distinguish the minor differences.

IV. EXPERIMENTS

We experimented to verify the features of the proposed model on simulator and real-world environments. The simulator experiment trained the model on an object position prediction task. Preciseness and sample efficiency were evaluated using datasets with different sizes (Fig. 3), along with comparisons against existing models. Whereas the real-world experiment focused on the proposed model and verified if it was applicable to noisy robot task settings. We trained it to predict object picking poses, which requires both image feature

TABLE II
SIMULATOR EXPERIMENT: AVERAGE ERROR DISTANCE IN CENTIMETERS. BOLDED BELOW 5CM

Prediction Target	Baseline Task						Top-down Task					
	Single Object			Multiple Objects			Selected Type			Selected Position		
Dataset size	4	20	100	4	20	100	4	20	100	4	20	100
Ours (q=min)	4.14	2.88	3.83	4.80	3.21	2.80	27.16	4.27	4.62	32.81	4.85	3.95
Key Point (q=16) [15]	2.16	3.69	0.62	22.41	3.85	2.61	33.28	24.61	7.94	31.82	15.75	9.63
Key Point (q=min) [15]	18.79	18.07	0.65	41.90	48.47	49.02	38.90	23.54	5.68	30.10	20.51	9.17
Deep Spatial AE (q=16) [5]	15.12	15.52	60.05	22.69	29.18	30.26	27.12	39.30	28.55	43.97	36.22	28.41
Convolutional AE	34.07	30.81	17.17	65.84	44.16	46.88	43.84	40.21	39.98	81.79	19.88	40.88
FCN	14.91	6.18	1.60	33.94	31.70	30.52	26.74	27.62	28.53	34.82	19.42	14.82

and coordinate data of attention points to determine how and where to perform the picking motion.

A. Environment configurations

For the simulator experiment, we employed a physics simulator called PyBullet [22] for environment simulations. As shown in Fig. 2(a), it was composed of a chequered floor and wooden textured table along with three types of objects: a duck figure, soccer ball, and mug. Each object was resized to a width of approximately 10 cm. The virtual camera was set to focus on the center of the table from a distance of 50 cm.

For the real-world experiment, we used IRB 14000 YuMi from ABB. This is a human collaborative dual-arm robot with seven degrees of freedom each and a gripper. As shown in Fig. 2(b), three objects were used for the tasks: a sponge, spray, and mug. A Realsense D435 RGBD camera was used for collecting RGB images, which was installed on top of the robot body.

B. Task settings

The general objective on both environments was to learn to recognize an object location. As shown in Table I, we derived four different tasks to break down and evaluate the ability. Tasks (a) and (b) comprised the baseline tasks and tasks (c) and (d) comprised the top-down tasks. Baseline tasks evaluates the model’s data efficiency. We trained the model to recognize the positions of all visible objects. In contrast, top-down tasks evaluated the model’s ability to predict positions of only a top-down specified target. Task (c) specified the object type, and task (d) specified whether the object is placed on the left or right side of the table.

C. Training configurations

The proposed model was trained to predict a minimum number of attention points that match the number of predicting objects (Table I). For query generation, the Base Queries and Conditioned Queries were used for the baseline tasks and top-down tasks, respectively. MLPs were used to convert attention coordinate values to object coordinates in simulator environment. Similarly, attention coordinate and feature values were concatenated and converted to robot picking poses with MLPs. The simulator and real-world tasks were trained to minimize the errors between the prediction and ground truth coordinate and robot pose values, respectively.

The proposed model was compared with existing visual attention models and vanilla FCN based models. The visual

attention models included “KeyPoint” model [15] and “Deep Spatial AE (Autoencoder)” [5]. Other attention models [2], [7] were excluded because they required specialized annotation or they are irrelevant to improving data efficiency. “Key Point” model [15] is composed of a vanilla FCN followed by a spatial softmax layer. Each image feature channel of the output is referred to as an attention heatmap and the coordinates of the most weighted pixels are output as the attention points. The model is tested on two conditions, in which the model was trained with the minimum (q=min) and redundant (q=16) number of attentions; “q” denotes the number of learned attention points. “Deep Spatial AE (Autoencoder)” [5] is an hourglass encoder-decoder model which employs the “KeyPoint” model as an encoder. In task (c) and (d), the one-hot vectors, that specify the targets, were input with the coordinates to convert to desired outputs using MLPs.

The vanilla FCN based models included “Convolutional AE” and vanilla “FCN”. “Convolutional AE” is an hourglass encoder-decoder model that employs convolutional layers and MLPs to compress an RGB image into a single vector. The compressed vector was input to MLPs for succeeding coordinate prediction.

V. EXPERIMENT RESULTS

A. Simulator experiment

Table II shows the experiment results on the simulator environment, along with the comparisons against existing vision models. The values are the average error distance between predicted and ground truth object coordinates. We bolded the values that had errors below 5cm, which is the half of the object width. Each model were evaluated on predictions with objects at 100 random positions.

1) *Proposed model*: Table II shows that the proposed model predicted object coordinates with a slight error under most conditions, when compared with other models. It is notable that the model retained high performance even on minimum training configurations, such as dataset size and the number of attentions. The predicted attention points on the untrained data are displayed in Fig. 4 (A). The points accurately located on the objects, which also suggests that the model adapted to appearance changes affected by the relative position to the camera. The proposed model succeeded on both top-down tasks (c) and (d), which indicates the model’s ability to specify targets based on appearances and spatial representations, namely feature-based attention and position-based attentions.

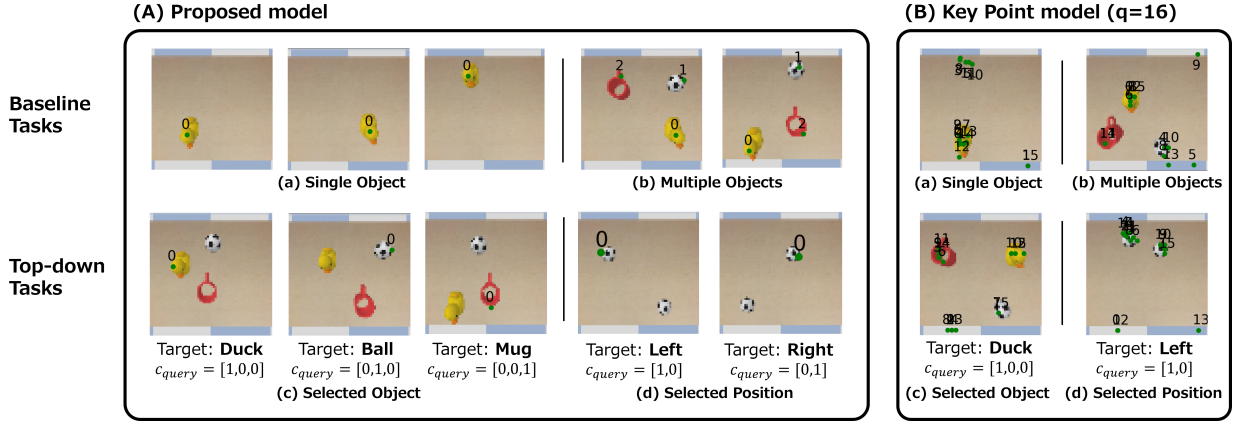


Fig. 4. (A) Visualization of predicted attention of the proposed model on simulator experiments. The green dots represent attention points, along with attention index numbers. (a)(b) Results of baseline tasks. (c)(d) Results of Top-Down tasks, each with different input conditions. (B) Visualization of attentions predicted by Key Point model (q=16) [15].

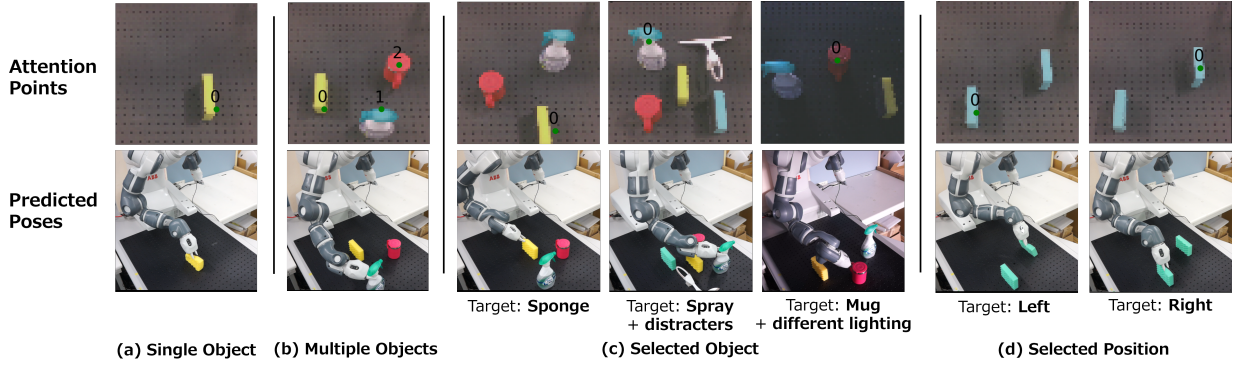


Fig. 5. Prediction results of real-world experiments. Top-row: visualization of attention points. Bottom-row: predicted robot poses for picking target objects.

However, when trained on dataset of size 4, the model failed to structure the queries for all target objects. The model predicted odd attention points, such as failing to acquire attention for one of three objects in task (c).

2) *Comparison models:* By contrast, Table II shows that Key Point models have lower sample efficiency: task (a) and (b) for KeyPoint (q=min) and task (b) for KeyPoint (q=16). Although Key Point models scored the highest when trained on the largest dataset in task (a), Fig. 4 (B) shows that some points attended to irrelevant locations, which decreases the interpretability. In addition, Fig. 4 (B) shows multiple points attending to different parts of a single object. This is because each attention heatmap only considers a single visual pattern, thus becomes vulnerable against minor appearance changes. Thus, the redundant number of attention points were necessary to increase the number of considered visual patterns.

Convolutional AE and Deep Spatial AE failed to predict on both of the baseline tasks. The reconstructed images showed images with background but no target objects. Considering the small space a single object occupied on the environment, the model is likely to have misinterpreted the object as a noise. This result suggests that separately training vision models induces a negative impact, especially when trained

on dataset with trivial visual stimulus. The results of FCN models indicated an increase in accuracy when provided with sufficiently dense datasets, which was as expected, considering the density of object positions in large datasets (Fig. 3).

All the existing models showed low precision on both top-down tasks. The Key Point model (q=16) had the best score among the compared models, which successfully attended to the presented objects (Figs. 4 (B) (c) and (d)). However, the model had less precision even when given a sufficient number of datasets and attention points. This is likely to be caused by the instability of the predicted attention points.

B. Real-world experiment

Table III shows the success rate of picking an object, each evaluated on 30 trials, where the target objects were placed at untrained positions. In Fig. 5, the top row shows the camera image with predicted attention points, and the bottom row shows the predicted robot poses. The model succeeded to direct the attention points to each target objects and to implicitly map the attention coordinates to real-world 3D coordinates to perform the picking motion. As shown in Fig. 5 (c), the model predicted different picking poses or approaching directions depending on the target object type. This result indicates that the model succeeded to distinguish the object

TABLE III
REAL-WORLD EXPERIMENT: SUCCESS RATE OF THE OBJECT PICKING

Task	Baseline Task		Top-down Task	
	Single Object	Multiple Objects	Selected Type	Selected Position
Dataset size	20	20	20	20
Success Rate	27/30	28/30	26/30	27/30

targets based on the jointly extracted image features. Although object types are actually given as conditions in this task, the ability to change predictions based on learned image features is essential to extend this model in the future works. The model also showed high robustness against noises, such as when presented with similar irrelevant objects or with darker lighting environments (Fig. 5 (c)). On the few failed trials (Table III), the model did succeed in predicting appropriate attention points, but the predicted gripper position tended to shift slightly. This occurred when the object appearance was affected by a strong distortion of the camera lenses, especially when placed at the edge of the environment.

VI. CONCLUSION

This paper presented a novel end-to-end learned top-down visual attention model. By separating the target representation to an independent Query vector, the model was able to guide the attention to different targets based on external input conditions. Experiments on simulation and real-world environments suggested that the model performed with high precision and interpretability even with minimum training configurations. In addition, introducing position-based attention and the feature extraction showed wider application capacity. However the model has limitations, where the model cannot automatically self-control the attention targets. Considering real-time robot controlling tasks, interaction targets are expected to change as the task proceeds. Therefore, we are currently working on expanding this model to employ such active top-down attention, in contrast to current static top-down attention.

ACKNOWLEDGMENT

This work was supported by JST Moonshot R&D Grant Number JPMJMS2031 and by JSPS KAKENHI Grant Number JP21H05138.

REFERENCES

- [1] Ashish Vaswani, Noam Shazeer, Niki Parmar, Jakob Uszkoreit, Llion Jones, Aidan N Gomez, Łukasz Kaiser, and Illia Polosukhin. Attention is all you need. *Advances in neural information processing systems*, 30, 2017.
- [2] Alexey Dosovitskiy, Lucas Beyer, Alexander Kolesnikov, Dirk Weissenborn, Xiaohua Zhai, Thomas Unterthiner, Mostafa Dehghani, Matthias Minderer, Georg Heigold, Sylvain Gelly, Jakob Uszkoreit, and Neil Houlsby. An image is worth 16x16 words: Transformers for image recognition at scale. In *International Conference on Learning Representations*, 2021.
- [3] Sanghyun Woo, Jongchan Park, Joon-Young Lee, and In So Kweon. Cbam: Convolutional block attention module. In *Proceedings of the European conference on computer vision (ECCV)*, pages 3–19, 2018.
- [4] Hengshuang Zhao, Jiaya Jia, and Vladlen Koltun. Exploring self-attention for image recognition. In *Proceedings of the IEEE/CVF Conference on Computer Vision and Pattern Recognition*, pages 10076–10085, 2020.
- [5] Chelsea Finn, Xin Yu Tan, Yan Duan, Trevor Darrell, Sergey Levine, and Pieter Abbeel. Deep spatial autoencoders for visuomotor learning. In *2016 IEEE International Conference on Robotics and Automation (ICRA)*, pages 512–519. IEEE, 2016.
- [6] Andy Zeng, Pete Florence, Jonathan Tompson, Stefan Welker, Jonathan Chien, Maria Attarian, Travis Armstrong, Ivan Krasin, Dan Duong, Vikas Sindhwani, et al. Transporter networks: Rearranging the visual world for robotic manipulation. *arXiv preprint arXiv:2010.14406*, 2020.
- [7] Daniel Seita, Pete Florence, Jonathan Tompson, Erwin Coumans, Vikas Sindhwani, Ken Goldberg, and Andy Zeng. Learning to rearrange deformable cables, fabrics, and bags with goal-conditioned transporter networks. In *2021 IEEE International Conference on Robotics and Automation (ICRA)*, pages 4568–4575. IEEE, 2021.
- [8] Robert Desimone and John Duncan. Neural mechanisms of selective visual attention. *Annual review of neuroscience*, 18(1):193–222, 1995.
- [9] Hideyuki Ichiwara, Hiroshi Ito, Kenjiro Yamamoto, Hiroki Mori, and Tetsuya Ogata. Spatial attention point network for deep-learning-based robust autonomous robot motion generation. *arXiv preprint arXiv:2103.01598*, 2021.
- [10] Zitong Liu, Quan Liu, Wenjun Xu, Zhihao Liu, Zude Zhou, and Jie Chen. Deep learning-based human motion prediction considering context awareness for human-robot collaboration in manufacturing. *procedia cirp*, 83:272–278, 2019. 11th cirp conference on industrial product-service systems.
- [11] Freek Stulp, Jonathan Grizou, Baptiste Busch, and Manuel Lopes. Facilitating intention prediction for humans by optimizing robot motions. In *2015 IEEE/RSJ International Conference on Intelligent Robots and Systems (IROS)*, pages 1249–1255, 2015.
- [12] Shaoqing Ren, Kaiming He, Ross Girshick, and Jian Sun. Faster r-cnn: Towards real-time object detection with region proposal networks. *Advances in neural information processing systems*, 28, 2015.
- [13] Joseph Redmon, Santosh Divvala, Ross Girshick, and Ali Farhadi. You only look once: Unified, real-time object detection. In *Proceedings of the IEEE conference on computer vision and pattern recognition*, pages 779–788, 2016.
- [14] Tejas Kulkarni, Ankush Gupta, Catalin Ionescu, Sebastian Borgeaud, Malcolm Reynolds, Andrew Zisserman, and Volodymyr Mnih. *Unsupervised Learning of Object Keypoints for Perception and Control*. curran associates inc., red hook, ny, usa, 2019.
- [15] Tomas Jakab, Ankush Gupta, Hakan Bilen, and Andrea Vedaldi. Unsupervised learning of object landmarks through conditional image generation. *Advances in neural information processing systems*, 31, 2018.
- [16] Youngrock Yoon, G.N. Desouza, and A.C. Kak. Real-time tracking and pose estimation for industrial objects using geometric features. In *2003 IEEE International Conference on Robotics and Automation (Cat. no.03ch37422)*, volume 3, pages 3473–3478 vol.3, 2003.
- [17] Menglong Zhu, Konstantinos G Derpanis, Yinfei Yang, Samarth Brahmabhatt, Mabel Zhang, Cody Phillips, Matthieu Lecce, and Kostas Daniilidis. Single image 3d object detection and pose estimation for grasping. In *2014 IEEE International Conference on Robotics and Automation (ICRA)*, pages 3936–3943. IEEE, 2014.
- [18] Hiroshi Ito, Kenjiro Yamamoto, Hiroki Mori, Shuki Goto, and Tetsuya Ogata. Visualization of focal cues for visuomotor coordination by gradient-based methods: A recurrent neural network shifts the attention depending on task requirements. In *2020 IEEE/SICE International Symposium on System Integration (SII)*, pages 188–194. IEEE, 2020.
- [19] Kei Kase, Chris Paxton, Hammad Mazhar, Tetsuya Ogata, and Dieter Fox. Transferable task execution from pixels through deep planning domain learning. In *2020 IEEE International Conference on Robotics and Automation (ICRA)*, pages 10459–10465. IEEE, 2020.
- [20] Rosanne Liu, Joel Lehman, Piero Molino, Felipe Petroski Such, Eric Frank, Alex Sergeev, and Jason Yosinski. An intriguing failing of convolutional neural networks and the coordconv solution. *Advances in neural information processing systems*, 31, 2018.
- [21] Francesco Locatello, Dirk Weissenborn, Thomas Unterthiner, Aravindh Mahendran, Georg Heigold, Jakob Uszkoreit, Alexey Dosovitskiy, and Thomas Kipf. Object-centric learning with slot attention. *Advances in Neural Information Processing Systems*, 33:11525–11538, 2020.
- [22] Erwin Coumans and Yunfei Bai. Pybullet, a python module for physics simulation for games, robotics and machine learning, 2016–2021.